

Increasing the Efficiency of Photocatalytic Water Treatment with Titanium Dioxide Nanoparticles by Control of Crystal Shape

D.G. Rickerby

European Commission Joint Research Centre, Institute for Environment and Sustainability,
21027 Ispra VA, Italy, david.rickerby@jrc.ec.europa.eu

ABSTRACT

Photocatalysis is increasingly applied for purification of drinking water and the treatment and recycling of industrial wastewater. The most common photocatalytic material is titanium dioxide; anatase is the photocatalytically reactive phase. However, the reaction itself is inherently inefficient because only a small fraction of the incident photons is actually used in photocatalysis. Various methods have been proposed to increase the efficiency, including doping with gold to increase the photocatalytic activity and doping with nitrogen or boron to extend the useable wavelengths into the visible range. Thermodynamic modelling indicates that, while decreasing particle size increases the specific surface area of the titanium dioxide, it reduces the percentage area of the photocatalytically active {001} facets. Recent work has been directed towards the controlled growth of titanium dioxide crystals with a greater proportion of high energy facets in order to increase the photocatalytic efficiency.

Keywords: photocatalysis, water treatment, nanoparticles, titanium dioxide

1 INTRODUCTION

Photocatalysis is emerging as an effective method both for degrading chemical pollutants [1] and the inactivation of bacteria [2, 3]. It can be used for purification of drinking water without chlorination and the treatment and recycling of industrial process water. Titanium dioxide is the most photocatalytically efficient material. It is a wide bandgap semiconductor, with $E_g = 3.2$ eV, and hence absorbs light wavelengths lower than 388 nm. The anatase phase is more photocatalytically reactive than rutile because most of the Ti atoms on the {001} surface are unsaturated with 5-fold coordination [4].

Less than 10% of the surface area of typical anatase nanocrystals consists of photocatalytically active facets. The present paper briefly outlines methods for increasing photocatalytic activity by doping and controlled growth of crystals and discusses how first principles thermodynamic modelling can lead to improved understanding of how the surface energy influences the morphology. It concludes by reviewing recent advances in synthesis of nanocrystals with a greater proportion of high energy facets to increase the photocatalytic efficiency.

2 PHOTOCATALYTIC MECHANISM

Photocatalysis takes place due to excitation of electrons from the valence band to the conduction band, by incident photons with energies greater than the band gap, leading to creation of electron-hole pairs (Figure 1). Electrochemical reactions with the acceptor and donor molecules (O_2 , H_2O) adsorbed on the surface of the semiconductor result in the formation of reactive ions (O_2^- , OH^\cdot), which are capable of degrading toxic organic compounds and destroying micro-organisms.

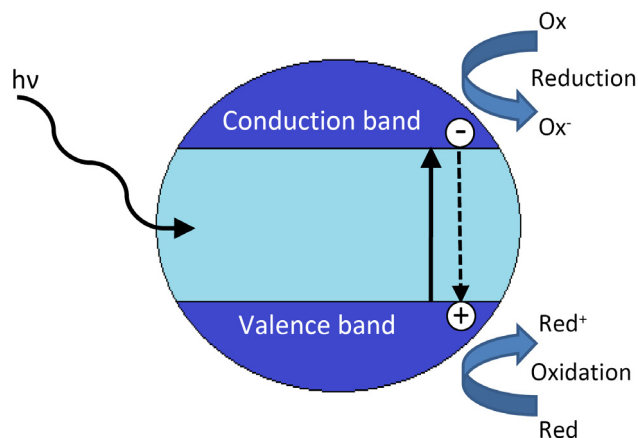
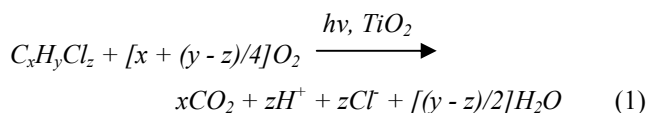


Figure 1: Schematic diagram of the photocatalytic reaction.

A generic equation for the photocatalytic oxidation of a chlorinated hydrocarbon can be written [5]



The photocatalytic reaction is inherently inefficient due to the effect of electron-hole recombination, which competes with reactions with donor and acceptor molecules, resulting in a non-linear dependence of the photonic efficiency on the photon reaction rate [6]. Generation of electrons and holes is therefore not sufficient alone to initiate the photocatalytic reaction. In addition, the electron-hole recombination rate must be low enough to allow adequate numbers of carriers to react with the adsorbed molecules on the surface of the oxide.

3 INCREASING PHOTOREACTIVITY

Various different techniques can be used to increase the efficiency of the photocatalytic reaction. Doping with low concentrations of metallic ions increases the photoreactivity by trapping charge carriers and preventing recombination [7]. Ultraviolet light constitutes only 5% of the spectrum of solar radiation, compared with approximately 46% for the visible wavelengths. Doping with Cr or V [8] and N and/or B [9, 10] can be used to narrow the band gap and extend the absorption band into the visible light range.

Quantum size effects influence the properties of very small nanoparticles. At a particle diameter of ~3 nm, gold loses its metallic character and begins to behave more like a semiconductor [11]. For concentrations of less than 1 at%, corresponding to gold particles of a bilayer thickness, the photocatalytic activity of TiO₂ is increased by a factor of greater than two [12].

Figure 2 shows commercially produced titanium dioxide nanoparticles of average diameter a few tens of nm with an irregular morphology and a large specific surface area [13]. However, according to the Wulff construction less than 6% of the total surface area of an anatase crystal is comprised of photoreactive {001} facets [14]. Current research is thus aimed at achieving controlled growth of TiO₂ nanocrystals with a higher fraction of these high energy surfaces.

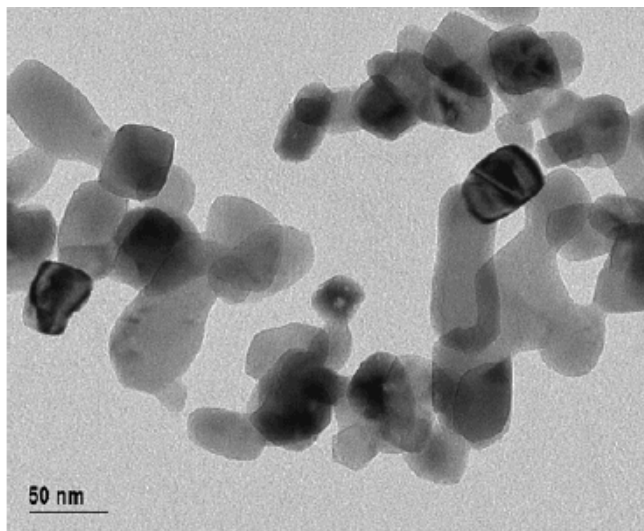


Figure 2: Transmission electron micrograph of dispersed anatase titanium dioxide nanoparticles

4 PARTICLE SHAPE CALCULATION

Calculation of the particle shape and phase stability by means of a thermodynamic model [15, 16] has indicated a dependence on particle size due to the increasing surface contribution to the free energy with decreasing size. This

model takes into account the variation of the free energy with crystal size and shape.

The total free energy is the sum of the bulk and surface contributions

$$G^0 = G^{bulk} + G^{surf} \quad (2)$$

The free energy of the nanocrystal is determined using the weighted sum of the contributions of the individual surfaces

$$G^0 = \Delta_f G^0 + M(1 - e)[q \sum_i f_i \gamma_i] / \rho \quad (3)$$

where $\Delta_f G^0$ is the free energy of formation of bulk material, M is the molar mass, e is the volume dilation due to surface tension, q is the surface to volume ratio, f_i is a weighting factor, γ_i is the surface energy of the surface i , and ρ is the density. The size dependence results from the increase in the surface to volume ratio and the volume dilation with decreasing crystal size. The shape dependence results from the increase in the surface to volume ratio and the increase in the surface free energy term.

The effective surface tension is the weighted sum over all crystal surfaces

$$\sigma = \sum_i f_i \sigma_i \quad (4)$$

The effective pressure due to surface tension is estimated using the Laplace-Young equation and the volume dilation due to surface tension is then

$$e = 2\beta\sigma / R \quad (5)$$

where R is the particle radius and β is the compressibility.

A numerical minimization procedure was employed to determine the crystal shape with the lowest free energy for a given nanoparticle size using values of γ_i and σ_i calculated by density functional theory for clean and hydrated low index surfaces of anatase and rutile TiO₂ [16]. The point of intersection of the free energies corresponds to the phase transition. Anatase is the thermodynamically stable phase for particle sizes below ~10 nm in vacuum and ~15 nm in water but metastable anatase can persist even for particle diameters much greater than this. For very small crystals (<3 nm diameter) the contribution due to edge and corner effects to the overall surface energy may also become significant [17].

Natural anatase crystals exhibit a truncated tetragonal bipyramidal form. This morphology may be described in terms of A , the side of the base of the pyramid, and B , the side of the square {001} truncation facets. The truncation is thus defined by the ratio B/A . Due to the size dependence of

the total free energy this ratio is smaller for nanocrystals than for larger size crystals. Simulated crystals based on the thermodynamic model and the standard Wulff construction are compared in Figure 3 (only the Ti atoms are shown for clarity). The shape predicted by the thermodynamic theory [18] corresponds closely to that of anatase nanoparticles synthesized under near-equilibrium conditions [19, 20].

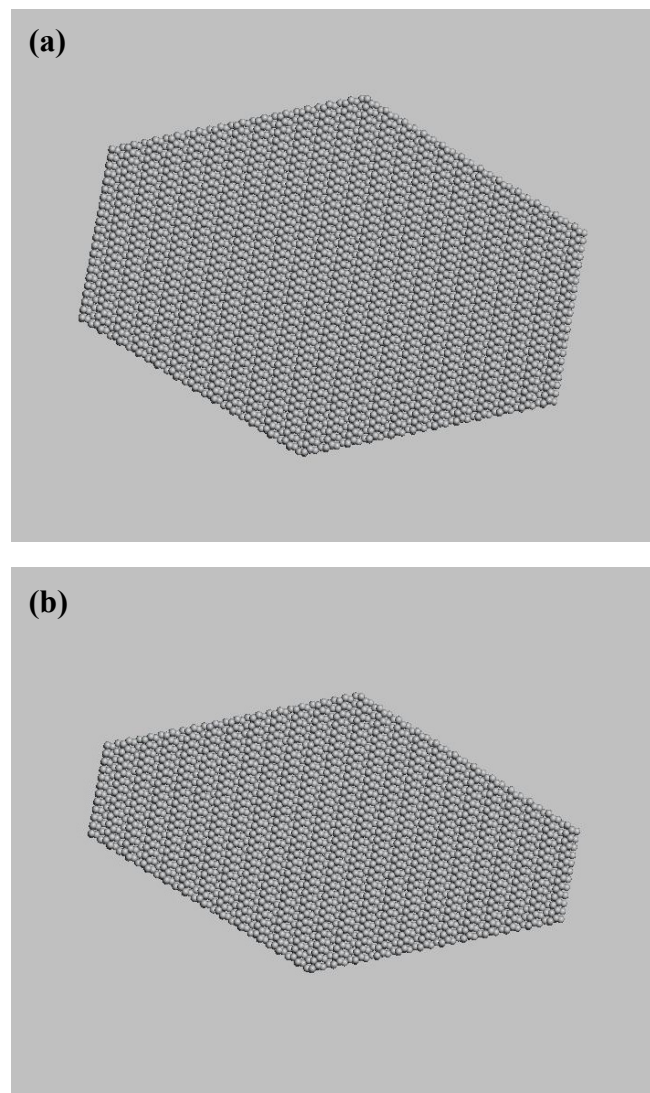


Figure 3: Simulated anatase titanium dioxide nanoparticles in the [100] projection: (a) Wulff construction; (b) lowest energy configuration based on the thermodynamic model.

5 CONTROLLED CRYSTAL GROWTH

Growth of stable $\{101\}$ facets is favoured with respect to reactive $\{001\}$ facets due to minimization of the total free energy. Decreasing the particle size thus increases the specific surface area, while at the same time reducing the overall fraction of the photoreactive $\{001\}$ facets. For this reason, reducing particle size may not be the most effective

means of increasing the photocatalytic efficiency and may indeed be counterproductive.

It is known that the pH value influences both particle size [21] and shape [22] in sol-gel preparation of titanium dioxide nanoparticles. Since γ_i and σ_i are sensitive to the surface state, B/A is dependent on whether the surface is hydrogenated, hydrated or oxygenated [23]. This gives the possibility of controlling crystal shape and phase stability by modification of the surface chemistry. Environmentally sensitive phase maps have been constructed based on the phase boundaries calculated applying the thermodynamic model [24].

Macroscopic ($\sim 1 \mu\text{m}$ diameter) anatase crystals with a higher percentage of reactive facets have been synthesized by dissolving titanium tetrafluoride in hydrofluoric acid diluted with deionized water and maintaining the solution at a temperature of 180°C for up to 20 hours [25]. Due to its low bonding energy, the presence of F strongly bound to Ti lowers the surface energy and thus promotes the growth of large $\{001\}$ facets. The degree of truncation of the crystals was found to depend on the pH of the solution. B/A ratios of up to 0.84, equivalent to a surface area consisting of 47% $\{001\}$ facets, were reported.

A non-aqueous method has been developed to produce anatase nanocrystals with an increased proportion of high energy facets, using titanium isopropoxide as the precursor [26]. The nanocrystals were of rhombic form and $\sim 10 \text{ nm}$ in size, with a large percentage of exposed high energy $\{010\}$ facets. They showed significantly increased photocatalytic efficiency compared with a commercial TiO_2 nanopowder, which was attributable to their superior absorbance due to the high percentage of exposed reactive facets. Due to the quantum confinement effect they also had a wider band gap (3.8 eV) than bulk anatase.

Anatase nanocrystals with a truncated bipyramidal form have been prepared by dissolving electrospun amorphous TiO_2 fibres in an aqueous acetic acid solution followed by hydrothermal treatment at 150°C for 20 hours [27]. Crystal morphology was dependent on the pH of the solution: 9.6% of the total surface area consisted of $\{001\}$ facets for a pH of 1.6, while reducing the pH to 0.23 tended to suppress the $\{001\}$ facets, resulting in a sharp tetragonal shape.

A solvothermal technique was used to produce a variety of nanocrystal morphologies including rhombic, truncated and elongated rhombic, spherical, dog-bone and bar shaped, from a titanium butoxide precursor [28]. Water vapour was used as the hydrolysis agent and oleic acid and oleylamine as capping surfactants to control crystal growth. The molar ratio of the surfactants played a critical role in determining the nanocrystal shape. Higher concentrations of oleic acid tended to suppress growth along $[011]$ directions by binding selectively to $\{001\}$.

Anatase nanocrystals have also been synthesized by an ionic liquid assisted hydrothermal method, using a TiCl_4 precursor and hydrofluoric acid or sulphuric acid to inhibit phase transformation and control shape [29]. Crystallization was dependent on the surfactant like properties of the ionic liquid, which influenced the aggregation behaviour. In the presence of HF the particle morphologies ranged from a square plate to a highly truncated bipyramidal shape, while H_2SO_4 resulted in a zigzag morphology, elongated along $\{001\}$, consisting of truncated pyramidal and parallelepiped components connected by common $\{001\}$ facets.

In general, nanocrystals synthesized by these methods tended to have a lower percentage of exposed $\{001\}$ facets than the macroscopic crystals. A possible solution to this limitation might lie in the use of hierarchical architectures, obtained for example with a low temperature hydrothermal process using Ti powders in an aqueous hydrofluoric acid solution [30]. This resulted in flower-like nanostructures 300-700 nm in diameter consisting of truncated tetragonal pyramidal TiO_2 with 50-150 nm $\{001\}$ exposed facets and $\{101\}$ sides.

6 CONCLUSION

Theoretical modelling can help provide insights on the influence of preferential growth of low energy facets and surface chemistry on nanocrystal shape. Enhancement of the photocatalytic efficiency requires not only reduction in particle size but also control of shape, including the use of hierarchical structures to increase the percentage of exposed reactive facets. Additional improvements in photoreactivity might be possible by combining techniques for controlled nanocrystal growth with nitrogen doping [31] to expand the absorption spectrum into the visible range.

REFERENCES

- [1] A. Mills and S. Le Hunte, *J. Photochem. Photobiol. A* 108, 1-35, 1997.
- [2] Z. Huang, P.-C. Maness, D.M. Blake, E.J. Wolfrum, S.L. Smolinski, W.A. Jakoby, *J. Photochem. Photobiol. A* 130, 163-170, 2000.
- [3] P.S.M. Dunlop, T.A. McMurray, J.W.J. Hamilton and J.A. Byrne, *J. Photochem. Photobiol. A* 196, 113-119, 2008.
- [4] M. Jacoby, *Chem. Eng. News* 86 (22), 12, 2008.
- [5] M.R. Hoffmann, S.T. Martin, W. Choi and D.W. Bahnemann, *Chem. Rev.* 95, 69-96, 1995.
- [6] D.W. Bahnemann, *Res. Chem. Intermed.* 26, 207-220, 2000.
- [7] S.I. Shah, W. Li, C-P. Huang, O. Jung and C. Ni, *Proc. Natl. Acad. Sci.* 99 (Suppl 2), 6482-6486, 2002.
- [8] M. Anpo, *Pure. Appl. Chem.* 72, 1787-1792, 2000.
- [9] S. In, A. Orlov, F. Garcia, M. Tikhov, D.S. Wright and R.M. Lambert, *Chem. Commun.* 40, 4236-4238, 2006.
- [10] S. In, A. Orlov, R. Berg, F. Garcia, S. Pedrosa-Jimenez, M.S. Tikhov, D.S. Wright and R.M. Lambert, *J. Am. Chem. Soc.* 129, 13790-13791, 2007.
- [11] M. Chen and D.W. Goodman, *Acc. Chem. Res.* 39, 739-746, 2006.
- [12] A. Orlov, D.A. Jefferson, M. Tikhov and R.M. Lambert, *Catal. Commun.* 8, 821-824, 2007.
- [13] D.G. Rickerby, *J. Mater. Ed.* 29, 95-106, 2007.
- [14] M. Lazzeri, A. Vittadini and A. Selloni, *Phys. Rev. B* 63, 155409, 2001.
- [15] A.S. Barnard and P. Zapol, *J. Phys. Chem. B* 108, 18435-18440, 2004.
- [16] A.S. Barnard, P. Zapol, and L. A. Curtiss, *J. Chem. Theory Comp.* 1, 107-116, 2005.
- [17] D.R. Hummer, J.D. Kubicki, P.R.C. Kent, J.E. Post and P.J. Heaney, *J. Phys. Chem. C* 113, 4240-4245, 2009.
- [18] D.G. Rickerby, *J. Nanosci. Nanotechnol.* 7, 1-8, 2007.
- [19] V. Shklover, T. Haibach, B. Bolliger, M. Hochstrasser, M. Erbudak, H.-U. Nissen, S.M. Zadeeruddin, Md.K. Nazeeruddin and M. Graetzel, *J. Sol. State. Chem.* 132, 60-72, 1997.
- [20] I. Djerdj, D. Arçon, Z. Jagličić, and M. Niederberger, *J. Solid State Chem.* 181, 1571-1581 2008.
- [21] T. Sugimoto, X. Zhou and A. Muramatsu, *J. Colloid Interface Sci.* 259, 43-52, 2003.
- [22] T. Sugimoto, X. Zhou and A. Muramatsu, *J. Colloid Interface Sci.* 259, 53-61, 2003.
- [23] A.S. Barnard and L. A. Curtiss, *Nano Lett.* 5, 1261-1266, 2005.
- [24] A. S. Barnard and H. Xu, *ACS Nano* 2, 2237-2242, 2008.
- [25] H.G. Yang, C.H. Sun, S.Z. Qiao, J. Zou, G. Liu, S.C. Smith, H.M. Cheng and G.Q. Lu, *Nature* 453, 638-641, 2008.
- [26] B. Wu, C. Guo, N. Zheng, Z. Xie and G.D. Stuckey, *J. Am. Chem. Soc.* 130, 17563-17567, 2008.
- [27] Y. Dai, C.M. Cobley, J. Zeng, Y. Sun and Y. Xia, *Nano Lett.* 9, 2455-2459, 2009.
- [28] C.-T. Dinh, T.-D. Nguyen, F. Kleitz and T.-O. Do, *ACS Nano* 3, 3737-3743, 2009.
- [29] K. Ding, Z. Miao, B. Hu, G. An, Z. Sun, B. Han and Z. Liu, *Langmuir* 26, 5129-5134, 2010.
- [30] M. Liu, L. Piao, W. Lu, S. Ju, L. Zhao, C. Zhou, H. Li and W. Wang, *Nanoscale* 2, 1115-1117, 2010.
- [31] G. Liu, H.G. Yang, X. Wang, L. Cheng, J. Pan, G.Q. Lu and H.-M. Cheng, *J. Am. Chem. Soc.* 131, 12868-12869, 2009.